



Soil carbon dynamics during drying vs. rewetting: Importance of antecedent moisture conditions

Kaizad F. Patel ^{a,*}, Allison Myers-Pigg ^{a,b}, Ben Bond-Lamberty ^c, Sarah J. Fansler ^a, Cooper G. Norris ^d, Sophia A. McKeever ^{a,e}, Jianqiu Zheng ^a, Kenton A. Rod ^f, Vanessa L. Bailey ^a

^a Biological Sciences Division, Pacific Northwest National Laboratory, Richland, WA, USA

^b Marine and Coastal Research Laboratory, Pacific Northwest National Laboratory, Sequim, WA, USA

^c Joint Global Change Research Institute, Pacific Northwest National Laboratory, College Park, MD, USA

^d Rochester Institute of Technology, Laboratory Science Technology, Rochester, NY, USA

^e Washington State University, Earth & Environmental Science, Richland, WA, USA

^f Washington State Department of Ecology, Richland, WA, USA

ARTICLE INFO

Keywords:

Soil organic matter
Carbon destabilization
Adsorption and desorption
Drying and rewetting

ABSTRACT

Soil moisture influences soil carbon dynamics, including microbial growth and respiration. The response of such ‘soil respiration’ to moisture changes is generally assumed to be linear and reversible, i.e. to depend only on the current moisture state. Current models thus do not account for antecedent soil moisture conditions when determining soil respiration or the available substrate pool. We conducted a laboratory incubation to determine how the antecedent conditions of drought and flood influenced soil organic matter (SOM) chemistry, bioavailability, and respiration. We sampled soils from an upland coastal forest, Beaver Creek, WA USA, and subjected them to drying and rewetting treatments. For the drying treatment, field moist soils were saturated and then dried to 75, 50, 35, and 5% saturation. In the rewetting treatment, field moist soils were air-dried and then rewet to 35, 50, 75, and 100% saturation. We measured respiration and water extractable organic carbon (WEOC) concentrations and used ¹H-NMR and FT-ICR-MS to characterize the WEOC pool across the treatments. The drying vs. wetting treatment strongly influenced SOM bioavailability, as rewet soils (with antecedent drought) had greater WEOC concentrations and respiration fluxes compared to the drying soils (with antecedent flood). In addition, air-dry soils had the highest WEOC concentrations, and the NMR-resolved peaks showed a strong contribution of protein groups in these soils. Both NMR and FT-ICR-MS analyses indicated increased contribution of complex aromatic groups/molecules in the rewet soils, compared to the drying soils. We suggest that drying introduced organic matter into the WEOC pool via desorption of aromatic molecules and/or by microbial cell lysis, and this stimulated microbial mineralization rates. Our work indicates that even short-term shifts in antecedent moisture conditions can strongly influence soil C dynamics at the core scale. The predictive uncertainties in current soil models may be reduced by a more accurate representation of soil water and C persistence that includes a mechanistic and quantitative understanding of the impact of antecedent moisture conditions.

1. Introduction

Soil moisture exerts strong physicochemical and biochemical controls on soil carbon (C) cycling, influencing substrate availability and access (Manzoni and Katul, 2014), altering microbial activity including heterotrophic respiration (Moyano et al., 2012). Under low-moisture conditions, there is a greater disconnect among soil pores, and microbial activity is limited by substrate diffusion. Greater hydrologic

connectivity improves microbial access to substrates, and consequently wet soils exhibit more soil respiration (Moyano et al., 2012; Yan et al., 2018).

The response of soil respiration, the surface-measured CO₂ flux produced by microbial respiration, to soil water content is typically assumed to follow a reversible and largely linear path. In reality, however, these responses can be strongly influenced by antecedent moisture conditions (Hawkes et al., 2020; Smith et al., 2017). The movement of

* Corresponding author.

E-mail address: kaizad.patel@pnnl.gov (K.F. Patel).

water in partially saturated soils is variable and hysteretic in nature, and depends, among other factors, on whether a soil is being wet or drained. For instance, as soils dry, water preferentially drains/evaporates from the macropores; on the other hand, capillary forces play a strong role during wetting, and micropores show greater hydrologic connectivity as soils are wet. Thus, soils at the same moisture content may experience different matric potentials, and different spatial distributions of water, depending on the antecedent conditions (Albers, 2014). Spatial access/discontinuity is an important mechanism of soil C protection, and as the soil moisture content changes, different pools of C, held in different pore size classes (Bailey et al., 2017) may be “activated” (Arnold et al., 2015), becoming available as potential substrates for microbial consumption and metabolism.

Antecedent moisture conditions can also influence the types of compounds present in the bioavailable C pool. As soils dry, the increasing ionic strength of shrinking water films stimulates desorption of aromatic compounds from mineral surfaces (Bailey et al., 2019; Kaiser et al., 2015). The high ionic stress can also impact microbial function, forcing increased production of stress osmolytes (Chowdhury et al., 2011), or even resulting in microbial cell lysis. Therefore, when dry soils are rewet, this newly destabilized-produced C would be available for microbial consumption. Indeed, the rewetting of dry soils is known to cause a flush of CO₂ (Birch, 1958), which has been linked to the physicochemical and biochemical mechanisms mentioned above (Bailey et al., 2019; Fierer and Schimel, 2003).

Although there seems to be an influence of antecedent moisture conditions, this has not been incorporated in soil C models, because we do not have a definitive understanding of the underlying mechanisms and changes occurring in soils during wetting vs. drying. Intensification of the global water cycle under current and predicted climate change scenarios suggests that drought, flooding, and water fluctuations will be more frequent in the future (Dai, 2012; Rahmstorf, 2017; Vousdoukas et al., 2018). Shifting hydrologic connectivities could mean changes in the protected vs. bioavailable pools of soil C, in turn influencing respiration and C loss from the soil. These changes potentially increase the importance of developing a mechanistic-based and thus predictive understanding of this ‘Birch effect’.

The objective of this study was to develop a molecular understanding of soil organic matter (SOM) dynamics occurring during drying and rewetting phases. We hypothesized that, compared to drying soils, soils that were rewet would have: (H1) greater CO₂ fluxes; (H2) greater availability of DOC; and (H3) more aromatic functional groups. We conducted a laboratory experiment where we incubated soils at various moisture levels, attained by drying of wet soils vs. rewetting of dry soils. We analyzed changes in the bioavailable C pool by measuring CO₂ flux and water extractable organic C (WEOC) and used ¹H-NMR and FT-ICR-MS to characterize molecular and functional changes in the WEOC pool due to the drying vs. rewetting treatments.

2. Methods

2.1. Site description and sampling

Soils were sampled from the Beaver Creek coastal watershed on the Washington coast (lat 46.907 N, lon 123.976 W). The watershed has an area of 3.8 km², with a salinity gradient from the tidal floodplains to the terrestrial upland forest (Sengupta et al., 2019; Yabusaki et al., 2020). The upland forest, where our samples were collected, is dominated by *Tsuga heterophylla* (western hemlock) trees with *Picea sitchensis* (sitka spruce). Soils are classified as medial, ferrhydritic, isomesic Typic Fulvudands (Mopang silt loam) (Soil Survey Staff, 2009). The surface litter was removed and soil was collected from the top 7 cm of the profile. Samples were brought back to the lab, sieved through 4 mm screens, and homogenized prior to further processing.

The sieved and homogenized soil was repacked into cores, 5 cm in diameter and 7.5 cm in height. Half the cores were repacked with

texture-unaltered soil (sandy clay loam), 30 g oven-dry equivalent, to a bulk density of 0.45 g/cm³ and 83.4% porosity. For the remaining half of the cores, we mixed 20 g oven-dry equivalent soil with 10 g Accusand® (Covia Corporation, OH, USA) to get a sandy loam texture (bulk density 0.60 g/cm³ and 77.1% porosity). Henceforth in this manuscript, we will refer to the two texture classes as SCL and SL.

2.2. Incubations

The cores were randomly assigned to one of two treatments, with five experimental replicates ($n = 5$) for each treatment-moisture-texture combination (Fig. 1).

Drying treatment: Soil cores were saturated (100% saturation) with deionized water on porous plates (SoilMoisture Equipment Corp.) and then dried down to 75, 50, 35, and 5% saturation (air-dry) by evaporative loss at 21 °C. When the soils reached their target weight (i.e., target moisture content), they were capped to prevent further loss and immediately incubated for 24 h in the dark at 21 °C. The drying process took ~30 h to five days, depending on the target weight, and the treatments were processed individually as soon as the weight was reached.

Rewetting treatment: Soils were air-dried (5% saturation) until constant weight, and then held at air-dry condition for one week. For the rewetting treatment, the soils were wet with deionized water to the same target moisture as in the drying treatment, i.e. 35, 50, 75, and 100% saturation. Wetting was done from above, using a syringe. The cores were capped to prevent evaporative loss and immediately incubated for 24 h in the dark at 21 °C.

2.3. Laboratory analyses

2.3.1. Soil respiration

During the 24-h incubation, the cores were connected to a Picarro G2301 Gas Concentration Analyzer (Picarro, Sunnyvale, CA, USA) with a 16-Port Distribution Manifold (Picarro A0311) for semi-continuous headspace CO₂ flux measurements. Fluxes were computed from the concentration changes according to the equation

$$A = (dC / dt * V / M * Pa / RT)$$

where A is the flux ($\mu\text{mol g soil}^{-1} \text{s}^{-1}$), dC/dt the rate of change in gas

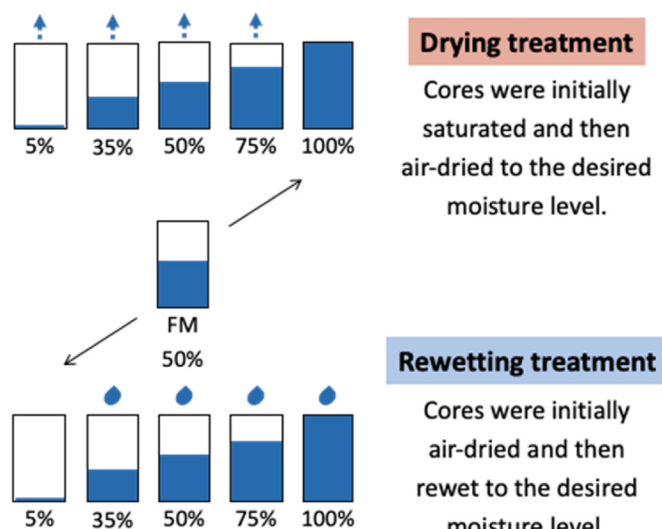


Fig. 1. Experimental design. For the *drying* treatment, soils were initially saturated and then dried to the desired moisture content. For the *rewetting* treatment, soils were initially air-dried and then rewet to the desired moisture content.

concentration (mole fraction s⁻¹), V the total chamber volume (cm³), M dry soil mass (g), Pa atmospheric pressure (kPa), R the universal gas constant (8.3×10^3 cm³ kPa mol⁻¹ K⁻¹), and T air temperature (K). Picarro data were processed using the *picarro*. *data* R package (Bond-Lamberty, 2020).

At the end of the incubation, the cores were deconstructed, the soils were homogenized in aluminum pans, and then immediately subsampled for the following analyses:

2.3.2. Gravimetric moisture

Gravimetric moisture was determined by placing soils in a forced-draft oven at 100 °C for 24 h, weighing them to the nearest 0.01 g, and calculated as:

$$\text{gravimetric moisture} = \frac{\text{field moist weight} - \text{oven dry weight}}{\text{oven dry weight}} \times 100\%$$

2.3.3. Water-extractable organic carbon (WEOC)

Organic carbon was extracted with Milli-Q deionized water (1:10 w/w) by shaking at 150 rpm at 4 °C for 16 h, centrifuging at 2000 g for 20 min, and then filtering through 0.45 µm polyethersulfone (PES) filters. Extracts were stored at 4 °C and WEOC was determined as non-purgeable organic carbon from combustion catalytic oxidation and nondispersive infrared (NDIR) detection using a Shimadzu TOC-L analyzer. The WEOC extract was processed for chemical characterization using solution state ¹H-NMR and FT-ICR-MS as complementary analytical techniques to identify the organic molecules (FT-ICR-MS) and functional groups (NMR) present in our extracts.

2.3.4. Nuclear magnetic resonance (NMR)

Ten mL of WEOC extract was freeze-dried and then stored under vacuum with phosphorus pentoxide (desiccant) to reduce residual water signals in the NMR spectra. The dried samples were reconstituted with 600 µL of DMSO-d₆ into 5 mm NMR tubes and analyzed on a Bruker 9.4 T 400 MHz Avance III NMR spectrometer with a BBFO 5 mm SmartProbe. One-dimensional ¹H NMR experiments were performed using 2720 scans and a recycle delay of 1 s. Spectral processing included phase and baseline correction, and spectral deconvolution through peak picking by the Global Deconvolution Model in MestreNova v14.1.2–25024 (Mestrelab Research). Peak intensities were normalized to the solvent.

Further processing was done using the *nmrr* package in R (Patel and Myers-Pigg, 2020), and the spectra were integrated into six regions following (Clemente et al., 2012): (1) aliphatic polymethylene and methyl groups (0.6–1.3 ppm, referred to as “aliphatic1” here); (2) aliphatic methyl and methylene near O and N (1.3–2.9 ppm, referred to as “aliphatic2” here); (3) O-alkyl, mainly from carbohydrates and lignin (2.9–4.1 ppm); (4) α-proton of peptides (4.1–4.8 ppm); (5) aromatic and phenolic (6.2–7.8 ppm); and (6) amide, from proteins (7.8–8.4 ppm). Integrations in each region were calculated as the sum of all peak areas within the region.

The relative abundance of each region was calculated as the proportion of the signal in each region to the total across all regions, normalized to 100%. As residual water peak (3.33 ppm) occupied most of the O-alkyl region in a non-uniform way across samples, we chose to disregard this region entirely in our analyses. This region represents primarily carbohydrate substituents. Peaks in the region 2.5–2.75 ppm were also disregarded, to avoid interference of the DMSO-d₆ solvent peaks.

2.3.5. Fourier-transform ion cyclotron resonance mass spectrometry (FT-ICR-MS)

The WEOC extracts were standardized to 25 ppm C and further purified by solid phase extraction (SPE). Samples were acidified to pH 2 with 85% phosphoric acid and then passed through Bond Elut PPL cartridges (Agilent Technologies) preactivated with CH₃OH. The

cartridges were washed three times with 10 mM HCl and then dried with N₂. The samples were eluted with 1.5 mL CH₃OH. The extracts were analyzed at the College of Sciences Major Instrumentation Cluster (COSMIC) laboratory at Old Dominion University, VA using negative-ion mode electrospray ionization with an Apollo II ion source on a Bruker 10 T APEX -Qe FT-ICR-MS. Due to unforeseen technical instrumental issues and the 2020 pandemic concerns, only the SCL samples were analyzed.

300 individual scans were averaged for each sample and internally calibrated using an organic matter homologous series separated by 14 Da (-CH₂ groups). The mass measurement accuracy was less than 1 ppm for singly charged ions across a broad m/z range (m/z 200–900). Data analysis software (Bruker Daltonik version 4.2) was used to convert raw spectra to a list of m/z values, and absolute intensity threshold set to the default value of 100. Chemical formulae were assigned using the Formularity program, including only peaks with a signal/noise ratio >7 (Kujawinski and Behn, 2006; Tolić et al., 2017), with the restrictions C₁₋₁₃₀, H₁₋₂₀₀, O₁₋₅₀, N₀₋₃, S₀₋₃, P₀₋₂.

Further processing was done using the *fticrr* package in R (Patel, 2020). FT-ICR-MS-resolved peaks were analyzed only on a presence/absence basis, due to established issues with intensities and ionization efficiencies in complex matrices using ESI (Kujawinski, 2002). Only peaks present in 3 or more replicates were considered present within that treatment. The peaks were assigned to one of the following classes following the method of Seidel et al. (2014, 2017): (1) polycyclic condensed aromatics (AI_{mod} > 0.66); (2) highly aromatic compounds, which include polyphenols and polycyclic aromatic compounds with aliphatic chains (0.66 > AI_{mod} > 0.50); (3) highly unsaturated compounds, which include phenols such as soil-derived products of lignin degradation (AI_{mod} < 0.50 and H/C < 1.5); and (4) aliphatic compounds (>H/C ≥ 1.5), including unsaturated aliphatics, N-containing aliphatics, and saturated compounds including fatty and sulfonic acids, and/or carbohydrates. The FT-ICR-MS compound classes are tentative classifications as they are solely based on the indices (O/C and H/C ratios and AI_{mod} values) from the molecular formula, not the molecular structure. Relative abundance values were calculated from count values associated with each observed biomolecule group normalized by the total number of C molecules identified.

2.4. Additional soil characterization

2.4.1. Water retention curves

Water retention curves (WRC) establish a relationship between water content and matric potential for a given soil. Drying phase water retention curves (Fig. 2) were produced for representative SCL and SL cores using a HYPROP-2 (METER Environment) and fit using the Van Genuchten function (Van Genuchten, 1980). The matric potential derived from the WRC is a function of the size of pore throats retaining the water (Carson et al., 2010; Marshall et al., 1996). A discussion of water release from different sized pores can be found in Appendix A1.

2.4.2. Total C and N

Soil was freeze-dried and analyzed for total C and total N in triplicate on a VarioMAX Cube (Elementar Analysensysteme GmbH), reported in Table 1.

2.4.3. Soil texture

Soil texture was determined using the hydrometer method of Gee and Bauder (1986). 50 g of sieved, dry soil was dispersed in 1 L deionized water with sodium hexametaphosphate in a hydrometer jar, and specific gravity measurements were performed with a hydrometer at 30 s, 2 h, and 24 h. The relative proportions of sand, silt, and clay fractions were calculated using standard formulae to determine the texture of the soil (Table 1).

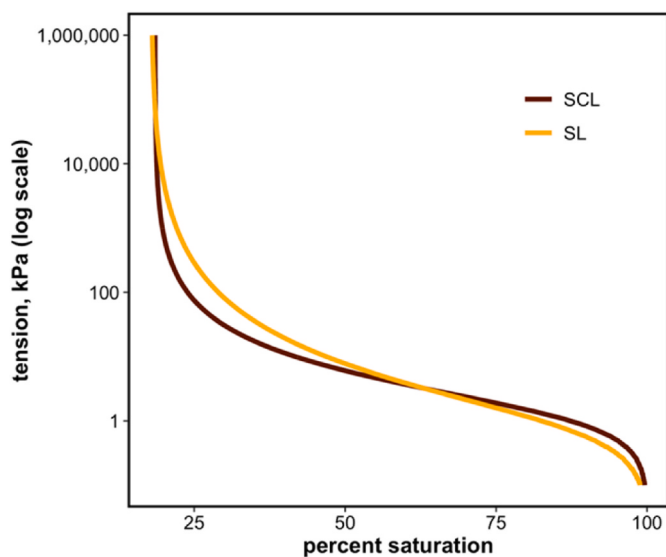


Fig. 2. Water retention curves for sandy clay loam (SCL) and sandy loam (SL) soils. Additional details are provided in Appendix A1.

Table 1
Characterization of Mopang soil used in this experiment.

Total C %	8.53
Total N %	0.33
C/N	25.85
% sand	46.08
% silt	25.37
% clay	28.56
texture	sandy clay loam

2.5. Data and statistical analysis

We used analysis of variance (ANOVA) to test the effect of antecedent conditions (drying vs. rewetting), moisture content, and texture on soil respiration and WEOC concentrations. We used permutational multivariate analysis of variance (PERMANOVA) and principal components analysis (PCA) to analyze FT-ICR-MS and NMR relative abundance data.

Additionally, we used Euclidean distances to determine relative effect sizes (drying vs. rewetting) for SCL and SL soils at different moisture contents. Statistical significance ANOVA and PERMANOVA was determined at $\alpha = 0.05$. All data analyses and visualization were performed in R version 4.0.2 (2020-06-02) (R Core Team, 2019), using primarily the *dplyr v1.0.1* (Wickham et al., 2020) and *vegan v2.5-6* (Oksanen et al., 2019) packages for data processing and analysis, and *ggplot2 v3.3.2* (Wickham, 2016) and *PNWColors* (Lawlor, 2020) packages for data visualization. All data and scripts are available at https://github.com/kaizadp/hysteresis_and_soil_carbon and archived on ESS-DIVE (<https://doi.org/10.15485/1764443>).

3. Results

3.1. Respiration and WEOC

Overall, CO₂ flux was influenced by treatment (ANOVA, $F = 29.83$, $p < 0.001$) and moisture content (ANOVA, $F = 135.86$, $p < 0.001$), but not by texture (ANOVA, $F = 1.60$, $p = 0.2090$). As expected, CO₂ flux was minimal (nearly zero) for the 5% saturated soils, and generally increased with moisture content up to 75% saturation (Fig. 3). For SCL, soils undergoing rewetting experienced significantly higher CO₂ fluxes than drying — this was seen across 50, 75, and 100% saturation conditions. For SL soils, a significant treatment effect was seen only for the 100% saturated soils.

WEOC concentrations were significantly influenced by treatment (ANOVA, $F = 188.68$, $p < 0.001$) and moisture (ANOVA, $F = 8.392$, $p = 0.005$), but not by texture (ANOVA, $F = 3.464$, $p = 0.07$). WEOC was greatest for soils at 5% saturation, ~2.6 times greater than that at other moisture levels (Fig. 4). Across almost all experimental units, rewetting soils had significantly greater WEOC than the drying soils (ANOVA, $p < 0.05$).

3.2. Molecular characterization of WEOC

3.2.1. FT-ICR-MS

The modified Van Krevelen classification of FT-ICR-MS-resolved peaks (based on molecular H/C and O/C ratios and Al_{mod}) showed that the field moist/control soils were dominated by highly unsaturated/lignin-like molecules (~64%), whereas simple aliphatic compounds accounted for ~18% of total peaks detected and identified. FT-ICR-MS-resolved WEOC peaks showed a significant influence of drying vs. rewetting treatment as well as moisture content (PERMANOVA,

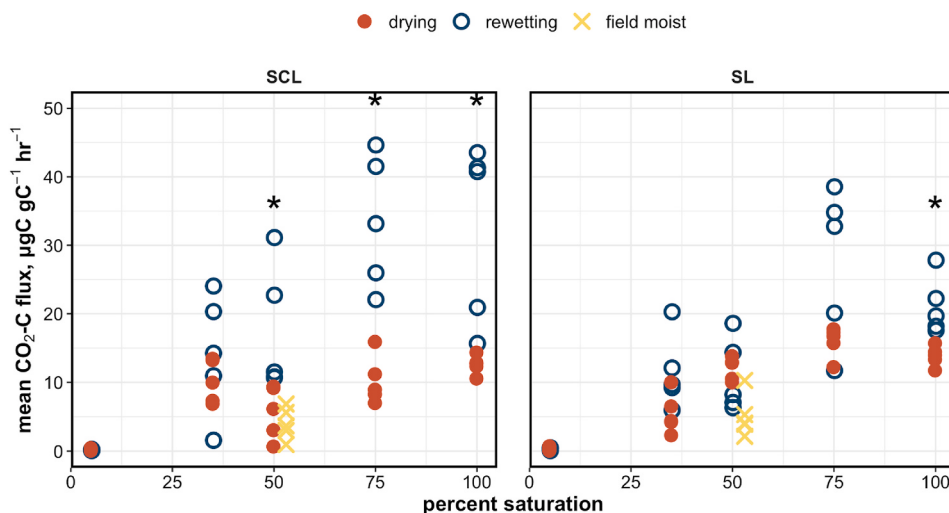


Fig. 3. Soil respiration (CO₂ flux) as a function of moisture content for sandy clay loam (SCL, left) and sandy loam (SL, right) textured soils. Respiration was low at air-dry conditions and generally increased with moisture content. Rewetting soils showed significantly greater respiration fluxes than drying soils. Asterisks represent significant differences between drying and rewetting phases at $\alpha = 0.05$.

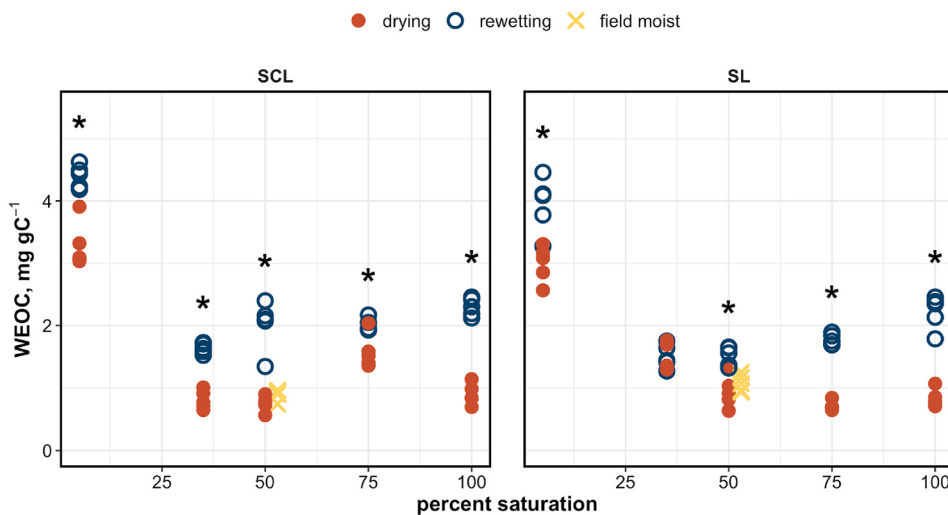


Fig. 4. Water extractable organic carbon (normalized to soil C content) as a function of soil moisture content. Air-dry soils had the greatest WEOC concentrations, and across most samples, WEOC concentrations were greater in rewetting soils than in drying. Asterisks denote significant differences between drying and rewetting phases at $\alpha = 0.05$.

interaction $F = 9.58$, $p = 0.002$). Principal components analysis (PCA) showed a strong separation by treatment — drying soils showed a stronger influence of simple aliphatic molecules, primarily for the 50–100% saturated soils (Fig. 5a). Rewet soils, on the other hand,

showed greater influence of complex molecules (aromatic and lignin-like). The rewetting soils also clustered more tightly than the drying soils.

To investigate the interaction between treatment and moisture level, we compared Euclidean distances between drying and rewetting cores (i.e., the magnitude of the treatment effect) across the five moisture levels — our analysis showed that the treatment effect was greatest for the 75% and 100% saturated soils (Fig. 5b).

Further analysis of peak counts showed that rewetting soils had a greater relative proportion of aromatic and lignin-like molecules, whereas the drying soils had a greater proportion of aliphatic molecules (Fig. 6).

3.2.2. NMR

NMR-resolved functional groups also showed significant effects of treatment (drying vs. rewetting, PERMANOVA, $F = 27.98$, $p < 0.001$), moisture ($F = 20.51$, $p < 0.001$), with a significant interaction between the two factors for SL soils ($p = 0.016$). Principal components analysis of these groups showed an overall separation by treatment — drying soils showed a greater influence of aliphatic peaks, whereas rewetting soils showed a greater influence of aromatic peaks (Fig. 7a). We compared Euclidean distances between drying and rewetting cores (i.e., the magnitude of the treatment effect) across the five moisture levels — our analysis showed that the treatment effect was greatest for 50% and 75% saturation in the sand-amended SL cores (Fig. 7b).

Consistent with the PCA results, a semi-quantitative analysis of relative abundance also indicated that the rewetting treatment increased the relative abundance of aromatic groups for many cores (Fig. 8). Protein α -H groups were absent (or minimally present) from all soils except the 5% saturated soils (air-dried), where they contributed 25–35% of total peak intensity.

A qualitative analysis of the NMR spectra indicated differences in the character of aromatic peaks for drying vs. rewetting soils. Peaks around 7.2 ppm were resolved into three distinct peaks for the drying soils, but a single peak for the rewetting soils. An example pair of spectra are presented in Fig. 9, to demonstrate the differences between the drying and rewetting treatments.

4. Discussion

4.1. Rewetting of dry soils increases available C

Our goal was to determine if drying vs. rewetting influenced soil C

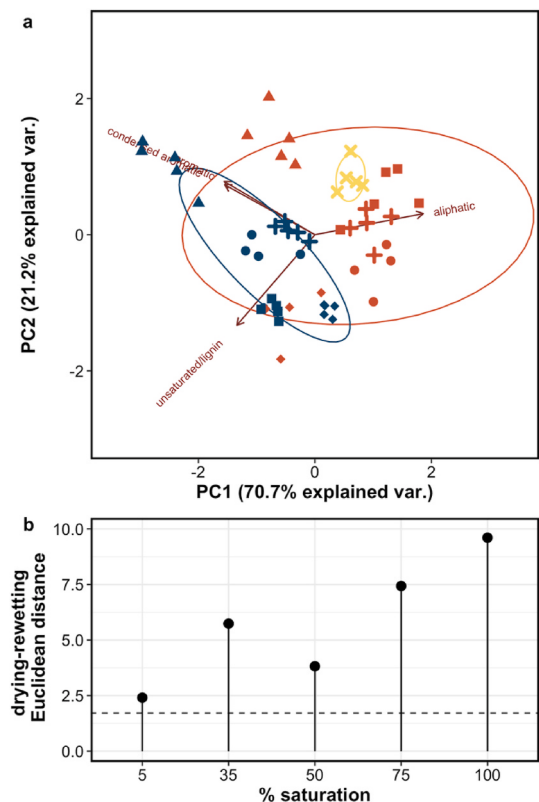


Fig. 5. (a) Principal components analysis (PCA) biplot FT-ICR-MS-resolved peaks in the sandy clay loam (SCL) samples. Drying soils showed a greater influence of aliphatic peaks, and rewetting soils showed a greater influence of aromatic and highly unsaturated, lignin-like peaks. The ellipses represent 95% confidence intervals. (b) Effect size of treatment (drying vs. rewetting) depicted as Euclidean distances for each moisture level. The horizontal dashed line is the average within-group distance, which represents the variability among replicates. The drying vs. rewetting treatment had greatest effect sizes for 75 and 100% saturated soils.

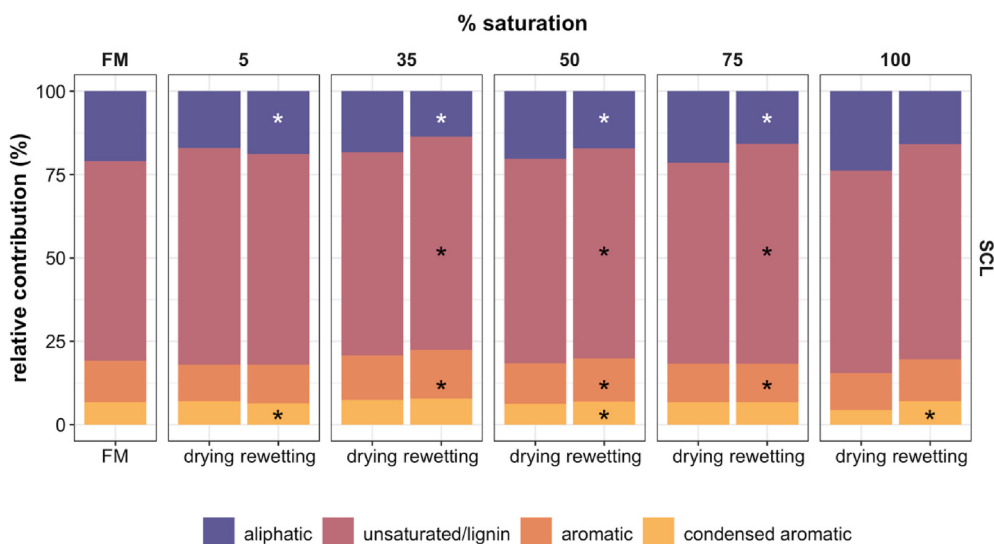


Fig. 6. Relative contribution of FT-ICR-MS-resolved peaks for the WEOC of sandy clay loam (SCL) samples. Drying soils had a greater contribution of aliphatic molecules, whereas rewetting soils had a greater relative contribution of complex aromatic and lignin-like molecules. Asterisks denote significant differences between drying and rewetting soils at $\alpha = 0.05$.

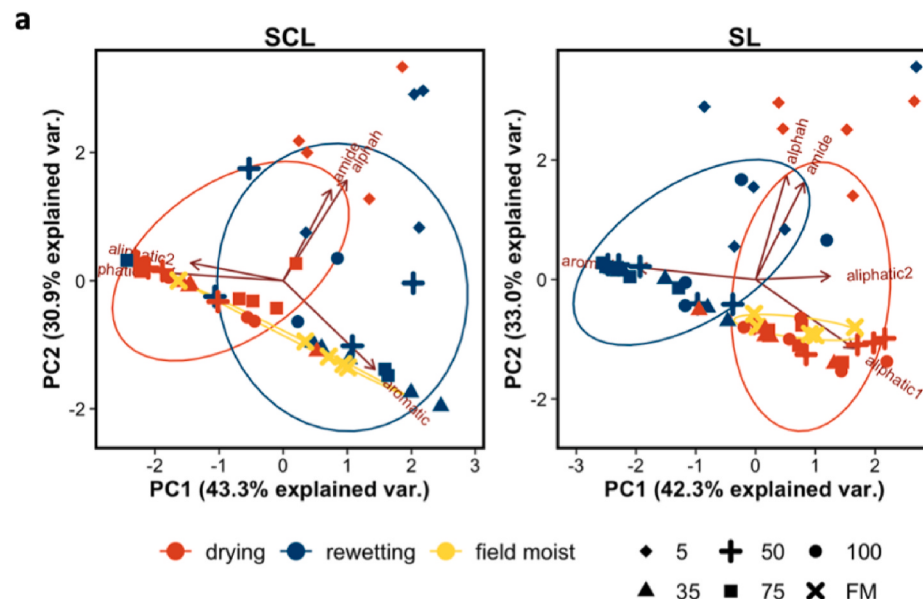
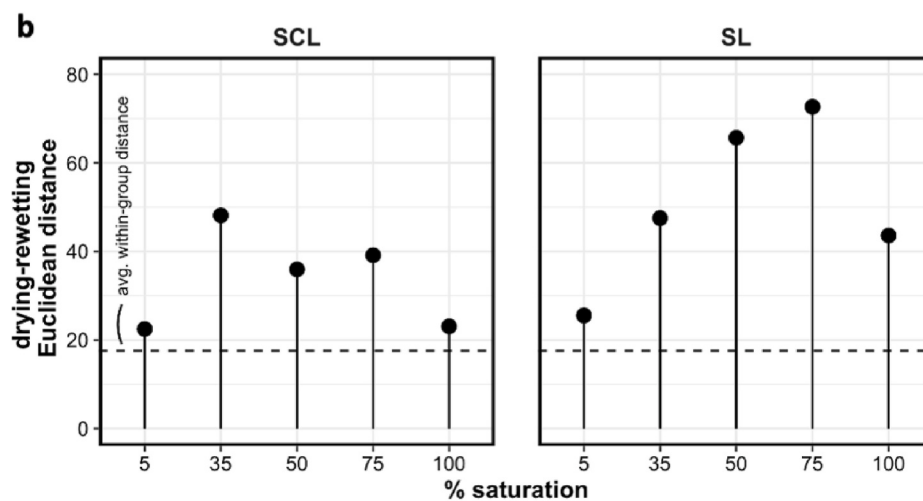


Fig. 7. (a) Principal components analysis (PCA) biplot of NMR-resolved groups in sandy clay loam (SCL) and sandy loam (SL) samples. The ellipses represent 95% confidence intervals. Air-dry soils showed greater influence of amides and proteins; drying soils showed greater influence of aliphatic groups; and rewetting soils showed greater influence of aromatic groups. (b) Effect size of treatment (drying vs. rewetting) depicted as Euclidean distances based on NMR-resolved relative abundances of sandy clay loam (SCL) and sandy loam (SL). The horizontal dashed line is the average within-group distance, which represents the variability among replicates. Drying vs. rewetting effect size was greater in sand-amended cores (sandy loam, SL), and was greatest for 50–75% saturated cores.



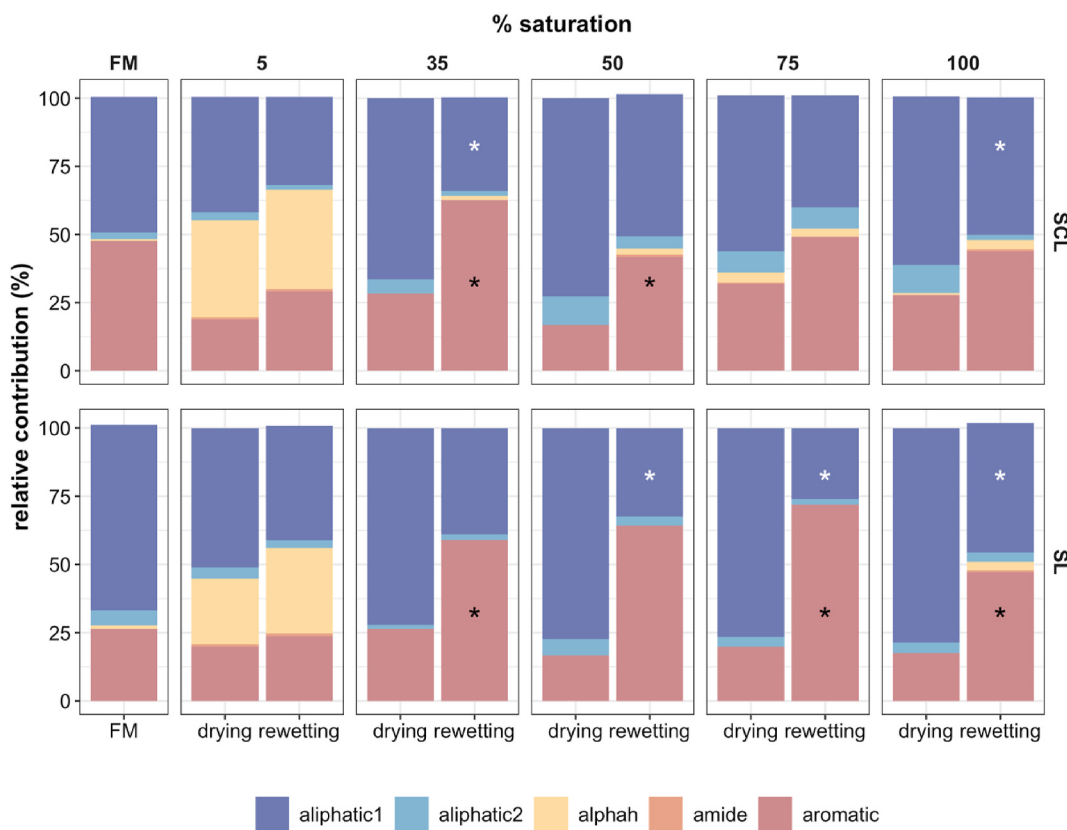


Fig. 8. Relative contribution of NMR-resolved groups to total intensity for sandy clay loam (SCL) and sandy loam (SL) samples. Air-dry soils had more protein groups; rewetting soils had more aromatic groups; and drying soils had more aliphatic groups. Asterisks denote significant differences between drying and rewetting treatments.

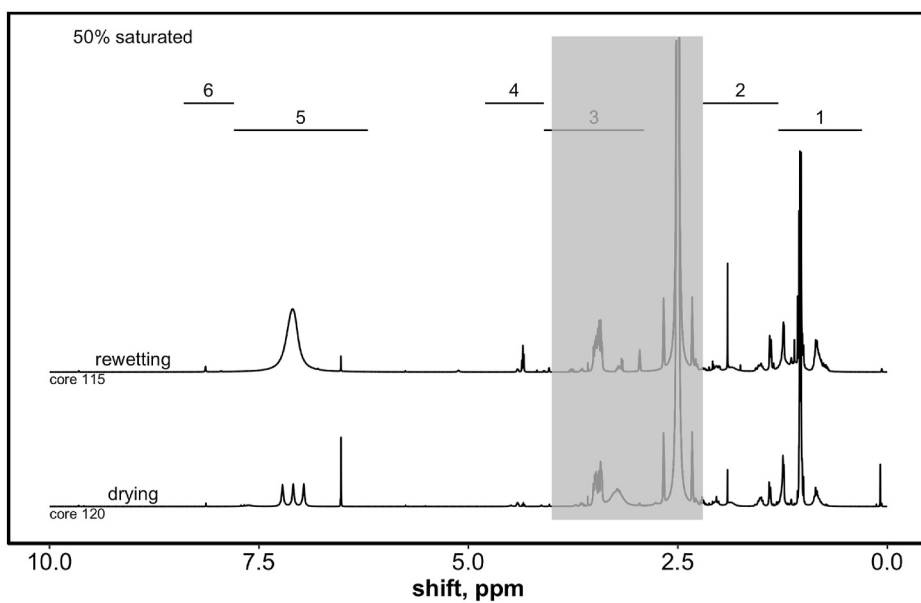


Fig. 9. Fitted and deconvoluted ^1H -NMR spectra for WEOC extracted from two SCL cores incubated at 50% saturation. Bins were obtained from Clemente et al. (2012): (1) aliphatic polymethylene and methyl groups (0.6–1.3 ppm, “aliphatic1”); (2) aliphatic methyl and methylene near O and N (1.3–2.9 ppm, “aliphatic2”); (3) O-alkyl, mainly from carbohydrates and lignin (2.9–4.1 ppm); (4) α -proton of peptides (4.1–4.8 ppm); (5) aromatic and phenolic (6.2–7.8 ppm); and (6) amide, from proteins (7.8–8.4 ppm). The grey region from 2.0 to 4.0 ppm includes solvent regions (DMSO-d_6 and H_2O) and is not included in the analyses. The peak at 2.50 ppm arises from the solvent (DMSO-d_6).

bioavailability, for soils held at the same moisture content. Core-scale metrics of carbon bioavailability-respiration and WEOC concentrations—showed a strong treatment effect, as rewetting of dry soils increased both CO_2 flux and WEOC concentrations compared to drying soils.

The high WEOC concentrations in our air-dry soils (5% saturation) suggest that a substantial amount of organic C became newly available

during the drying process. The WEOC declined as these air-dry soils were subsequently rewet, with a corresponding increase in CO_2 production, suggesting that the newly available C may have been consumed and mineralized as hydrologic pore connectivity increased. This phenomenon — increased WEOC and the resultant pulse of CO_2 seen upon rewetting (i.e., the Birch effect) (Birch, 1958; Jarvis et al., 2007) — is largely driven by physicochemical and biochemical processes occurring

in the soil. Destabilization of adsorbed/protected C increases the pool of C potentially available for microbes (Bailey et al., 2019). Additionally, microbial inputs (mortality) may also increase the bioavailable pool of C, caused by microbial cell lysis from drought stress (Blazewicz et al., 2014), or increased enzyme activity due to substrate-induced enzyme production (Fierer and Schimel, 2003; Halverson et al., 2000).

The FT-ICR-MS and ¹H-NMR results offer insights into the molecular changes that resulted from these treatments, and we see two major responses:

Increased amino acid content in air-dry soils: the air-dry (5% saturated) soils had a high abundance of α -H from amino acids (seen in NMR spectra). Amino acids in soil are typically derived from microbial biomass (Kallenbach et al., 2015), and have been used as a biomarker for microbial necromass (Amelung, 2001; Joergensen, 2018; Liang et al., 2019; Miltner et al., 2012). While we cannot conclusively trace the origins of these peaks in our study, it is possible that the amino groups in the air-dry soils may have been derived from microbial origin, and possibly entered the soil due to cell lysis. Since these peaks were not as abundant in the other experimental units (and in many cases, not even detected), these amino groups were likely rapidly consumed and metabolized when the dry soils were rewet, contributing at least partly to the CO₂ flush seen in the rewetting soils.

Increased aromatic content in rewetting soils: rewetting of dry soils increased the relative proportion of aromatic groups and molecules (seen in both NMR and FT-ICR-MS). We expected an increased presence of aromatic compounds in the WEOC of rewetting soils, because drying causes desorption of aromatic species from mineral surfaces (Newcomb et al., 2017), and these results support our hypothesis. The NMR results for the air-dry soils show a muted response of aromatic groups and appear to contradict this pattern. However, these contrasting results may be explained by two possible mechanisms: (a) the newly available protein groups in the air-dry soils stimulated respiration, and preferential metabolism of aliphatic compounds caused a relative enrichment of the aromatic groups; or (b) drying did cause desorption of aromatic groups, but this was masked by the greater increase in protein groups seen during the drying process. The shifting relative abundance of aromatic groups as a result of wetting/drying is coupled with a shift in the composition within the grouping. The NMR peak at 7.2 ppm is indicative of aromatic amino acids, (Clemente et al., 2012), and the differences in peak resolution/complexity at this position (Fig. 9) suggest that wetting/drying affects not only the relative abundance of these high-level functional groups, but also the diversity of molecules within these groups.

4.2. Soil moisture and spatial access

Soil respiration showed a strong dependence on soil water content, increasing with moisture and peaking at ~75% saturation, consistent with our general understanding of soil water-respiration dynamics (Moyano et al., 2012; Yan et al., 2018). Under partially saturated conditions, discontinuous resource islands are formed in the soil, and microbes have limited access to substrates. As soils are wet, hydrologic connectivity increases microbial access to substrates in different pore throats (Arnold et al., 2015), stimulating C mineralization. Beyond optimal moisture contents, the microbes become oxygen-limited, resulting in lower respiration rates in saturated or nearly saturated soils.

Our analyses of FT-ICR-MS-resolved peaks also suggest an influence of moisture on molecular composition of the WEOC pool (Fig. 5a and b). Soils incubated at 75 and 100% saturation showed the strongest effect (separation) of drying vs. rewetting soils, and it is possible that the increased hydrologic connectivity in the rewet soils may have stimulated microbial processing of the recently added substrate. It is also important to note that osmotic potential in the soils would increase suddenly as the dry soils were rewet. As the osmotic “upshift” would be greater for 75% and 100% saturation, these soils could have experienced greater cell lysis (i.e., greater additions of microbial necromass),

contributing to the greater drying vs. wetting differences at higher water content (Kieft et al., 1987). The drying soils at 50–100% moisture clustered tightly in the aliphatic region, separated from the 35% and 5% saturated soils – suggesting that as soils continued drying beyond 50% saturation (6–7 kPa), it may have stimulated the desorption of lignin-like and aromatic molecules from the pores in the 8–50 μ m range (Appendix A1).

Water retention curves help us understand the distribution of water in pores, as the matric potential is a function of the size of pore throats retaining the water (Carson et al., 2010; Marshall et al., 1996). Generally, soils along the drying curve experience greater matric tensions than soils along the wetting curve (Albers, 2014), and as a result, the water in drying soils is generally held in smaller pore throats than in wetting soils, even at the same water content. In other words, for a given saturation level, water-filled porosity (i.e., hydrological connectivity), and therefore substrate availability would also be greater in wetting soils compared to drying. This may have also contributed to greater respiration in wetting soils. Similarly, as different pore sizes are wet, different pools of C may be available for microbial consumption. Bailey et al. (2017) demonstrated that pore throats >200 μ m were dominated by lipids and other easily decomposed C substrates, whereas fine pores (6–20 μ m) were dominated by complex C compounds (aromatic, lignin-like, and tannin-like). Our soil cores in this experiment were homogenized, and therefore we can expect some redistribution of pore sizes as well as the organic compounds across different pore size classes. These pore-scale differences may be more important in intact soils in the field, where DOC is more likely to be fractionated by pore sizes.

Addition of sand in the SL cores introduced more macropores, and although the size of pores wet did not change much between the two soil types (Appendix A1), the SL soils held less total water (and thus, more air) in their pores compared to SCL soils, for similar saturation levels. This could reduce hydrologic connectivity of pores in SL soils, which may explain why the SL cores showed a noticeably stronger drying vs. rewetting in the ¹H-NMR spectra (Fig. 8). However, it is unlikely that the spatial distribution of organic compounds was significantly altered, since the addition of sand introduced immediate and artificial macropores, compared to the naturally formed and weathered macropores that occur in non-manipulated sandy loam soils. Soil texture may therefore play a stronger role in SOM dynamics in naturally occurring soils (Cable et al., 2008).

4.3. Utility of complementary analyses

This study also demonstrates the utility of multiple complementary analytical techniques for SOM characterization. While ultra-high-resolution FT-ICR-MS is valuable in determining changes in the types of molecules present, the ¹H-NMR allowed us to identify shifts in molecular functionality of groups, such as amides and proteins, that are not detected by FT-ICR-MS. The NMR results also indicate that proteins and aromatic amino acids are major players in the SOM cycling occurring during wetting/drying cycles, highlighting the need to investigate N-containing compounds further. Finally, flux measurements from the soil surface provide an integrative measure of microbial activity, as well as a crucial link with field-scale fluxes; such measurements are frequently made in natural and managed ecosystems worldwide (Jian et al., 2020).

4.4. Implications

Our results demonstrate the strong influence of antecedent moisture conditions on soil C dynamics. Both respiration and WEOC concentrations showed a hysteretic, non-reversible relationship with soil water content, driven by the drying vs. rewetting phase the soils were experiencing. We suggest that drought may have a stronger impact on soil C cycling than flooding, since drying may irreversibly alter the bioavailable SOM pool via chemical changes to the soil organic C molecules, sorption-desorption reactions, and microbial cell lysis. Conversely,

short-term soil anoxia from flooding seems to be quickly reversible.

The long-term moisture and disturbance history of a site are also known to influence soil C cycling (Hawkes et al., 2020), since microbes or their functions may adapt to the site-specific conditions over time (Bond-Lamberty et al., 2016). However, our experiment focuses on short-term antecedent moisture conditions, for which we assume the microbes have not had time to adapt to the stress conditions. Instead, changes in C mineralization are driven more by physico-chemical mechanisms of SOM destabilization, microbial functional potential, and biochemical response to the extent of microbial cell lysis.

With the intensification of the global water cycle, soil moisture fluctuations are expected to become more frequent and intense (Grillakis, 2019; Prein et al., 2017; Trenberth et al., 2014), and it is becoming increasingly important to understand the effect this will have on soil C persistence or, destabilization, and mineralization. Current soil C models predict C mineralization based on singular moisture measurements that are translated into simple and invertible mathematical functions, though this may not be reflective of real-world processes (Ghezzehei et al., 2019; Moyano et al., 2013). But current predictive uncertainties may be reduced by a more accurate representation of soil water and C persistence that includes a mechanistic and quantitative understanding of the impact of antecedent moisture conditions. Our work suggests that antecedent moisture conditions may be particularly important when considering transformations at the core scale, as rewetting of dry soils mobilizes more C than drying of wet soils. While the mechanisms discussed here would likely be seen in other soil systems as well, the magnitudes of C mobilization and efflux would also depend on factors like intensity and duration of drought and frequency of drying-rewetting cycles, as well as long-term climate history (Fierer and Schimel, 2002; Hoover and Rogers, 2016; Meisner et al., 2015; Sawada et al., 2017). A number of studies have suggested that these dynamics

are important at the field scale as well, however, particularly under generally water-limited (Cable et al., 2013) or elevated CO₂ conditions (Ryan et al., 2015). Given that precipitation extremes are likely to increase with ongoing climate change (Dai, 2012; Rahmstorf, 2017; Vousdoukas et al., 2018), new mechanistic and modeling studies are needed to investigate these effects at larger scales, using a range of integrating techniques to fully characterize and understand the underlying processes.

Data availability

All data and scripts are available at https://github.com/kaizadp/hysteresis_and_soil_carbon and archived on ESS-DIVE (Patel et al. 2021. <https://doi.org/10.15485/1764443>).

Declaration of competing interest

The authors declare that they have no known competing financial interests or personal relationships that could have appeared to influence the work reported in this paper.

Acknowledgments

We thank Marci Garcia, Lupita Renteria, and Josh Torgeson for assistance with laboratory processing of samples. We thank Vivian Lin for assistance with NMR setup. This research was supported by the U.S. Department of Energy, Office of Science, Biological and Environmental Research as part of the Terrestrial Ecosystem Sciences Program. The Pacific Northwest National Laboratory is operated for DOE by Battelle Memorial Institute under contract DE-AC05-76RL01830. We thank Don Lentz for access to the Beaver Creek field site.

Appendix

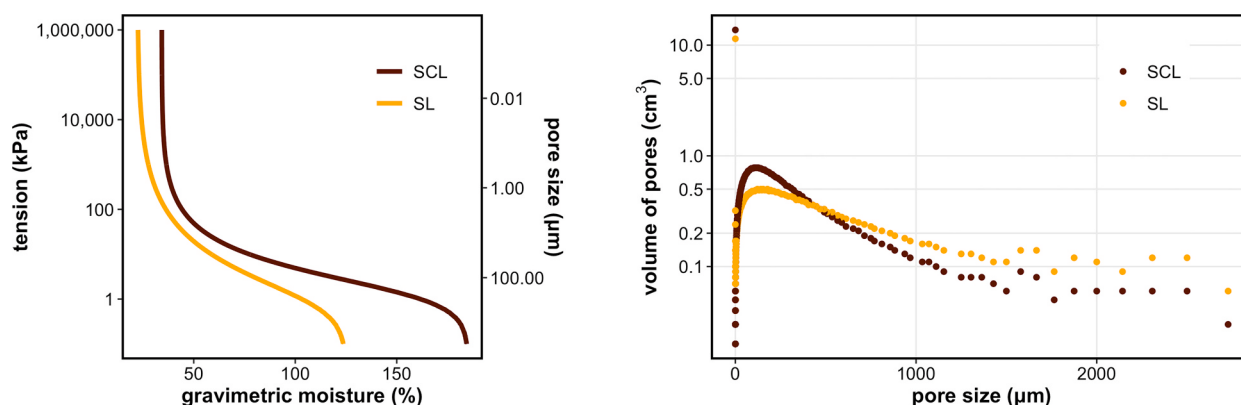
A1. Pore size distribution from in SCL and SL cores

The Kelvin equation for perfectly wettable soils describes the relationship between the size of water-filled pores and the water potential applied to a soil core (Carson et al., 2010; Marshall et al., 1996), and it can be reduced to:

$$\text{diameter of the largest water-filled pore } (\mu\text{m}) = \frac{300}{\text{water potential } (\text{kPa})}$$

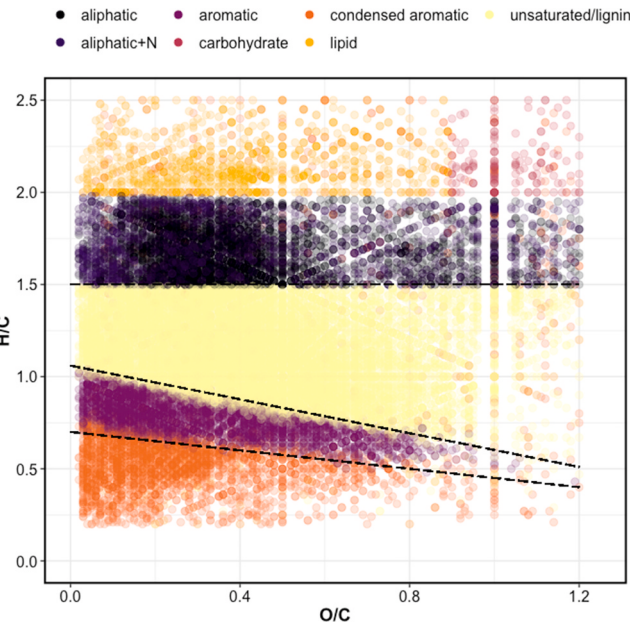
The first panel shows the water retention curve, similar to Fig. 2 in the main text, but the water content is reported in terms of gravimetric moisture. Overall, SL soils held less water in their pores compared to SCL soils.

We applied the Kelvin equation to the water potentials in the water retention curves (Fig. 2) to calculate the size of water-filled pore throats as SCL and SL soils dried over seven days. We calculated the volume of water successively released, and the figure below describes the volume of water released by different sized pores. We see that a substantial portion of soil water was held in pores <0.1 μm.



A2. Functional domains of FT-ICR-MS resolved molecules

Van Krevelen plots describe FT-ICR-MS-resolved peaks in terms of the molecular H:C and O:C ratios. We classified the peaks into seven groups using a modified Van Krevelen classification, following Seidel et al. (2014, 2017): (1) polycyclic condensed aromatics ($\text{AI}_{\text{mod}} > 0.66$); (2) highly aromatic compounds, which include polyphenols and polycyclic aromatic compounds with aliphatic chains ($0.66 > \text{AI}_{\text{mod}} > 0.50$); (3) highly unsaturated compounds, which include phenols such as soil-derived products of lignin degradation ($\text{AI}_{\text{mod}} > 0.50$ and $\text{H/C} < 1.5$); and (4) aliphatic compounds ($\text{H/C} \geq 1.5$ and $\text{N} = 0$); (5) aliphatic compounds containing N ($\text{H/C} \geq 1.5$ and $\text{N} > 0$); (6) saturated lipid-like compounds ($\text{H/C} \geq 2.0$ and $\text{O/C} < 0.9$); (7) saturated carbohydrate-like compounds ($\text{H/C} \geq 2.0$ and $\text{O/C} \geq 0.9$).



References

- Albers, B., 2014. Modeling the hysteretic behavior of the capillary pressure in partially saturated porous media: a review. *Acta Mechanica* 225, 2163–2189. <https://doi.org/10.1007/s00707-014-1122-4>.
- Amelung, W., 2001. Methods using amino sugars as markers for microbial residues in soil, in: *Assessment Methods for Soil Carbon*. Lewis Publishers Boca Raton 233–270.
- Arnold, C., Ghezzehei, T.A., Berhe, A.A., 2015. Decomposition of distinct organic matter pools is regulated by moisture status in structured wetland soils. *Soil Biology and Biochemistry* 81, 28–37. <https://doi.org/10.1016/j.soilbio.2014.10.029>.
- Bailey, V.L., Pries, C.H., Lajtha, K., 2019. What do we know about soil carbon destabilization? *Environmental Research Letters: ERL* [Web Site] 14, 083004. <https://doi.org/10.1088/1748-9326/ab2c11>.
- Bailey, V.L., Smith, A.P., Tfaily, M., Fansler, S.J., Bond-Lamberty, B., 2017. Differences in soluble organic carbon chemistry in pore waters sampled from different pore size domains. *Soil Biology and Biochemistry* 107, 133–143. <https://doi.org/10.1016/j.soilbio.2016.11.025>.
- Birch, H.F., 1958. The effect of soil drying on humus decomposition and nitrogen availability. *Plant and Soil* 10, 9–31. <https://doi.org/10.1007/BF01343734>.
- Blazewicz, S.J., Schwartz, E., Firestone, M.K., 2014. Growth and death of bacteria and fungi underlie rainfall-induced carbon dioxide pulses from seasonally dried soil. *Ecology* 95, 1162–1172.
- Bond-Lamberty, B., 2020. *picarro.data: Parse and Compute on Picarro Analyzer Files*.
- Bond-Lamberty, B., Bolton, H., Fansler, S., Heredia-Langner, A., Liu, C., McCue, L.A., Smith, J., Bailey, V.L., 2016. Soil respiration and bacterial structure and function after 17 years of a reciprocal soil transplant experiment. *PloS One* 11. <https://doi.org/10.1371/journal.pone.0150599>.
- Cable, J.M., Ogle, K., Barron-Gafford, G.A., Bentley, L.P., Cable, W.L., Scott, R.L., Williams, D.G., Huxman, T.E., 2013. Antecedent conditions influence soil respiration differences in shrub and grass patches. *Ecosystems* 16, 1230–1247. <https://doi.org/10.1007/s10021-013-9679-7>.
- Cable, J.M., Ogle, K., Williams, D.G., Weltzin, J.F., Huxman, T.E., 2008. Soil texture drives responses of soil respiration to precipitation pulses in the sonoran desert: implications for climate change. *Ecosystems* 11, 961–979. <https://doi.org/10.1007/s10021-008-9172-x>.
- Carson, J.K., Gonzalez-Quiñones, V., Murphy, D.V., Hinz, C., Shaw, J.A., Gleeson, D.B., 2010. Low pore connectivity increases bacterial diversity in soil. *Applied and Environmental Microbiology* 76, 3936–3942. <https://doi.org/10.1128/AEM.03085-09>.
- Chowdhury, N., Marschner, P., Burns, R., 2011. Response of microbial activity and community structure to decreasing soil osmotic and matric potential. *Plant and Soil* 344, 241–254.
- Clemente, J.S., Gregorich, E.G., Simpson, A.J., Kumar, R., Courtier-Murias, D., Simpson, M.J., 2012. Comparison of nuclear magnetic resonance methods for the analysis of organic matter composition from soil density and particle fractions. *Environmental Chemistry* 9, 97–107. <https://doi.org/10.1071/EN11096>.
- Dai, A., 2012. Increasing drought under global warming in observations and models. *Nature Climate Change* 3, 52–58. <https://doi.org/10.1038/nclimate1633>.
- Fierer, N., Schimel, J.P., 2002. Effects of drying-rewetting frequency on soil carbon and nitrogen transformations. *Soil Biology and Biochemistry* 34, 777–787. [https://doi.org/10.1016/S0038-0717\(02\)00007-X](https://doi.org/10.1016/S0038-0717(02)00007-X).
- Fierer, N., Schimel, J.P., 2003. A proposed mechanism for the pulse in carbon dioxide production commonly observed following the rapid rewetting of a dry soil. *Soil Science Society of America Journal* 67, 798. <https://doi.org/10.2136/sssaj2003.0798>.
- Gee, G.W., Bauder, J.W., 1986. Particle-size analysis. *Methods of Soil Analysis: Part 1 Physical and Mineralogical Methods* 5, 383–411.
- Ghezzehei, T.A., Sulman, B., Arnold, C.L., Bogie, N.A., Berhe, A.A., 2019. On the role of soil water retention characteristic on aerobic microbial respiration. *Biogeosciences* 16, 1187–1209.
- Grillakis, M.G., 2019. Increase in severe and extreme soil moisture droughts for Europe under climate change. *The Science of the Total Environment* 660, 1245–1255. <https://doi.org/10.1016/j.scitotenv.2019.01.001>.
- Halverson, L.J., Jones, T.M., Firestone, M.K., 2000. Release of intracellular solutes by four soil bacteria exposed to dilution stress. *Soil science society of America journal*. *Soil science society of America. SSSA Special Publication* 9 (64), 1630–1637. <https://doi.org/10.2136/sssaj2000.6451630x>.
- Hawkes, C.V., Shinoda, M., Kivlin, S.N., 2020. Historical climate legacies on soil respiration persist despite extreme changes in rainfall. *Soil Biology and Biochemistry* 143, 107752. <https://doi.org/10.1016/j.soilbio.2020.107752>.
- Hoover, D.L., Rogers, B.M., 2016. Not all droughts are created equal: the impacts of interannual drought pattern and magnitude on grassland carbon cycling. *Global Change Biology* 22, 1809–1820. <https://doi.org/10.1111/gcb.13161>.
- Jarvis, P., Rey, A., Petsikos, C., Wingate, L., Rayment, M., Pereira, J., Banza, J., David, J., Miglietta, F., Borghetti, M., Manca, G., Valentini, R., 2007. Drying and wetting of Mediterranean soils stimulates decomposition and carbon dioxide emission: the “Birch effect.” *Tree Physiology* 27, 929–940. <https://doi.org/10.1093/treephys/27.7.929>.

- Jian, J., Vargas, R., Anderson-Teixeira, K., Stell, E., Herrmann, V., Horn, M., Kholod, N., Manzon, J., Marchesi, R., Paredes, D., Bond-Lamberty, B., 2020. A restructured and updated global soil respiration database (SRDB-V5). Data, Algorithms, and Models. <https://doi.org/10.5194/essd-2020-136>.
- Joergensen, R.G., 2018. Amino sugars as specific indices for fungal and bacterial residues in soil. *Biology and Fertility of Soils* 54, 559–568. <https://doi.org/10.1007/s00374-018-1288-3>.
- Kaiser, M., Kleber, M., Berhe, A.A., 2015. How air-drying and rewetting modify soil organic matter characteristics: an assessment to improve data interpretation and inference. *Soil Biology and Biochemistry* 80, 324–340. <https://doi.org/10.1016/j.soilbio.2014.10.018>.
- Kallenbach, C.M., Grandy, A.S., Frey, S.D., Diefendorf, A.F., 2015. Microbial physiology and necromass regulate agricultural soil carbon accumulation. *Soil Biology and Biochemistry* 91, 279–290. <https://doi.org/10.1016/j.soilbio.2015.09.005>.
- Kieft, T.L., Soroker, E., Firestone, M.K., 1987. Microbial biomass response to a rapid increase in water potential when dry soil is wetted. *Soil Biology and Biochemistry* 19, 119–126. [https://doi.org/10.1016/0038-0717\(87\)90070-8](https://doi.org/10.1016/0038-0717(87)90070-8).
- Kujawinski, E.B., 2002. Electrospray ionization fourier transform ion cyclotron resonance mass spectrometry (ESI FT-ICR MS): characterization of complex environmental mixtures. *Environmental Forensics* 3, 207–216. <https://doi.org/10.1080/713848382>.
- Kujawinski, E.B., Behn, M.D., 2006. Automated analysis of electrospray ionization fourier transform ion cyclotron resonance mass spectra of natural organic matter. *Analytical Chemistry* 78, 4363–4373. <https://doi.org/10.1021/ac0600306>.
- Lawlor, J., 2020. PNWColors: color palettes inspired by nature in the US Pacific Northwest. Zenodo. <https://doi.org/10.5281/ZENODO.3971032>.
- Liang, C., Amelung, W., Lehmann, J., Kästner, M., 2019. Quantitative assessment of microbial necromass contribution to soil organic matter. *Global Change Biology* 25, 3578–3590. <https://doi.org/10.1111/gcb.14781>.
- Manzoni, S., Katul, G., 2014. Invariant soil water potential at zero microbial respiration explained by hydrological discontinuity in dry soils. *Geophysical Research Letters* 41, 7151–7158. <https://doi.org/10.1002/2014GL061467>.
- Marshall, T.J., Holmes, J.W., Rose, C.W., 1996. *Soil Physics*. Cambridge University Press.
- Meisner, A., Rousk, J., Bååth, E., 2015. Prolonged drought changes the bacterial growth response to rewetting. *Soil Biology and Biochemistry* 88, 314–322. <https://doi.org/10.1016/j.soilbio.2015.06.002>.
- Miltner, A., Bombach, P., Schmidt-Bücken, B., Kästner, M., 2012. SOM genesis: microbial biomass as a significant source. *Biogeochemistry* 111, 41–55. <https://doi.org/10.1007/s10533-011-9658-z>.
- Moyano, F.E., Manzoni, S., Chenu, C., 2013. Responses of soil heterotrophic respiration to moisture availability: an exploration of processes and models. *Soil Biology and Biochemistry* 59, 72–85. <https://doi.org/10.1016/j.soilbio.2013.01.002>.
- Moyano, F.E., Vasilyeva, N., Bouckaert, L., Cook, F., Craine, J., Curiel Yuste, J., Don, A., Epron, D., Formanek, P., Franzluebbers, A.J., Ilstedt, U., Kätterer, T., Orchard, V., Reichstein, M., Rey, A., Ruamps, L., Subke, J.A., Thomsen, I.K., Chenu, C., 2012. The moisture response of soil heterotrophic respiration: interaction with soil properties. *Biogeosciences* 9, 1173–1182. <https://doi.org/10.5194/bg-9-1173-2012>.
- Newcomb, C.J., Qafoku, N.P., Grate, J.W., Bailey, V.L., De Yoreo, J.J., 2017. Developing a molecular picture of soil organic matter–mineral interactions by quantifying organo–mineral binding. *Nature Communications* 8, 396. <https://doi.org/10.1038/s41467-017-00407-9>.
- Oksanen, J., Blanchet, F.G., Friendly, M., Kindt, R., Legendre, P., McGlinn, D., Minchin, P.R., O'Hara, R.B., Simpson, G.L., Solymos, P., Others, 2019. *Vegan: Community Ecology Package (R Package Version 2.5–5)*; 2019.
- Patel, K.F., 2020. kaizadp/fticrrr: FTICR-results-in-R. <https://doi.org/10.5281/zenodo.3893246>.
- Patel, K.F., Myers-Pigg, A., 2020. kaizadp/nmrrr: first release. <https://doi.org/10.5281/zenodo.3858839>.
- Prein, A.F., Rasmussen, R.M., Ikeda, K., Liu, C., Clark, M.P., Holland, G.J., 2017. The future intensification of hourly precipitation extremes. *Nature Climate Change* 7, 48–52. <https://doi.org/10.1038/nclimate3168>.
- Rahmstorf, S., 2017. Rising hazard of storm-surge flooding. *Proceedings of the National Academy of Sciences of the United States of America*. <https://doi.org/10.1073/pnas.1715895114>.
- R Core Team, 2019. *R: A Language and Environment for Statistical Computing*.
- Ryan, E.M., Ogle, K., Zelikova, T.J., LeCain, D.R., Williams, D.G., Morgan, J.A., Pendall, E., 2015. Antecedent moisture and temperature conditions modulate the response of ecosystem respiration to elevated CO₂ and warming. *Global Change Biology* 21, 2588–2602. <https://doi.org/10.1111/gcb.12910>.
- Sawada, K., Funakawa, S., Kosaki, T., 2017. Effect of repeated drying–rewetting cycles on microbial biomass carbon in soils with different climatic histories. *Applied Soil Ecology: a Section of Agriculture, Ecosystems & Environment* 120, 1–7. <https://doi.org/10.1016/j.apsoil.2017.07.023>.
- Seidel, M., Beck, M., Riedel, T., Waska, H., Suryaputra, I.G.N.A., Schnetger, B., Niggemann, J., Simon, M., Dittmar, T., 2014. Biogeochemistry of dissolved organic matter in an anoxic intertidal creek bank. *Geochimica et Cosmochimica Acta* 140, 418–434. <https://doi.org/10.1016/j.gca.2014.05.038>.
- Seidel, M., Manecki, M., Herlemann, D.P.R., Deutsch, B., Schulz-Bull, D., Jürgens, K., Dittmar, T., 2017. Composition and transformation of dissolved organic matter in the Baltic Sea. *Frontiers of Earth Science* 5, 31. <https://doi.org/10.3389/feart.2017.00031>.
- Sengupta, A., Indivero, J., Gunn, C., Tfaily, M.M., Chu, R.K., Toyoda, J., Bailey, V.L., Ward, N.D., Stegen, J.C., 2019. Spatial gradients in the characteristics of soil-carbon fractions are associated with abiotic features but not microbial communities.
- Smith, A.P., Bond-Lamberty, B., Benscoter, B.W., Tfaily, M.M., Hinkle, C.R., Liu, C., Bailey, V.L., 2017. Shifts in pore connectivity from precipitation versus groundwater rewetting increases soil carbon loss after drought. *Nature Communications* 8, 1335. <https://doi.org/10.1038/s41467-017-01320-x>.
- Soil Survey Staff, 2009. Natural resources conservation service, United States department of agriculture. Web Soil Survey. <http://websoilsurvey.sc.egov.usda.gov/>.
- Tolić, N., Liu, Y., Liyu, A., Shen, Y., Tfaily, M.M., Kujawinski, E.B., Longnecker, K., Kuo, L.-J., Robinson, E.W., Paša-Tolić, L., 2017. Formularity: software for automated formula assignment of natural and other organic matter from ultrahigh-resolution mass spectra. *Analytical Chemistry* 89, 12659–12665. <https://doi.org/10.1021/acs.analchem.7b03318>.
- Trenberth, K.E., Dai, A., van der Schrier, G., Jones, P.D., Barichivich, J., Briffa, K.R., Sheffield, J., 2014. Global warming and changes in drought. *Nature Climate Change* 4, 17–22. <https://doi.org/10.1038/nclimate2067>.
- Van Genuchten, M.T., 1980. A closed-form equation for predicting the hydraulic conductivity of unsaturated soils 1. *Soil Science Society of America Journal* 44, 892–898. <https://doi.org/10.2136/sssaj1980.03615995004400050002x>.
- Voudoukas, M.I., Mentaschi, L., Voukouvalas, E., Verlaan, M., Jevrejeva, S., Jackson, L.P., Feyen, L., 2018. Global probabilistic projections of extreme sea levels show intensification of coastal flood hazard. *Nature Communications* 9, 2360. <https://doi.org/10.1038/s41467-018-04692-w>.
- Wickham, H., 2016. *ggplot2: Elegant Graphics for Data Analysis*. Springer.
- Wickham, H., François, R., Henry, Lionel, 2020. *Dplyr: a grammar of data manipulation*.
- Yabusaki, S.B., Myers-Pigg, A.N., Ward, N.D., Waichler, S.R., Sengupta, A., Hou, Z., Chen, X., Fang, Y., Duan, Z., Serkowski, J.A., Indivero, J., Wiese Moore, C., Gunn, C.M., 2020. Floodplain inundation and salinization from a recently restored first-order tidal stream. *Water Resources Research* 56, 196. <https://doi.org/10.1029/2019WR026850>.
- Yan, Z., Bond-Lamberty, B., Todd-Brown, K.E., Bailey, V.L., Li, S., Liu, C., Liu, C., 2018. A moisture function of soil heterotrophic respiration that incorporates microscale processes. *Nature Communications* 9, 1–10. <https://doi.org/10.1038/s41467-018-04971-6>.